Crack growth behavior of SBR, NR and BR rubber compounds: comparison of Pure-Shear versus Strip Tensile test

G. Andreini, P. Straffi, S. Cotugno

Bridgestone Technical Center Europe, via del fosso del Salceto 13-15, 00128 Roma - ITALY

G. Gallone, G. Polacco

Department of Civil and Industrial Engineering, University of Pisa, Largo Lucio Lazzarino 1, 56122 Pisa - ITALY

ABSTRACT

Fatigue crack growth experiments on different carbon black–filled rubber compounds have been carried out to evaluate the influence of pure-shear and strip tensile testing mode by using sine and pulse as waveforms. In a previous set of experimental investigations regarding the influence of both waveform and tested material, it was found that the mode I of crack opening sometimes propagates too quickly to be properly monitored in tests involving strip-tensile specimens. An alternative test methodology based on pure-shear test mode has been investigated, optimizing both the shape of the specimen and the test equipment. Data obtained from the different compound formulations were consistent with the theoretical background and resulted in similar ranking of compound crack growth resistance for the two testing modes; in addition, pure-shear mode showed a higher sensitivity to formula variations.

Keywords: Rubber, Crack propagation, SENT, Pure Shear, Waveform,

INTRODUCTION

Rubber products may undergo fatigue phenomena during their service life. The effect of waveform on crack propagation in rubber products using different sample geometries was investigated by various authors.[1–8] A specific contribution to this task was given by Mars et al.,[1,2] who considered pulse waveform and multiaxial specimen as the most appropriate representation of the strain history in a tire. On the other hand, Hardy et al.[3] found that crack resistance behavior of rubber products under sine waveform depends not only on the polymer

but also on other compounding variables such as filler type and content.

Although the effect of different waveforms on crack propagation was investigated by Harbour et al.,[4] who determined the effect of dwell time using different sine wave cycles, a comparison between pure-shear and a single-edge notched tension (SENT) specimen using a real pulse waveform was not investigated. In a previous contribution,[9] the authors showed that fatigue crack growth determination with strip-tensile tests has some limitations; a typical case was a polybutadiene rubber (BR) compound in which the crack propagated faster than the maximum allowed frame rate of the video acquisition system, so that data could not be acquired at all.

The purpose of this investigation is to clarify the influence of different sample geometries on rubber crack propagation as well as the effect of different waveforms on compound formulations that differ only in polymer type.

BACKGROUND

Modern fatigue tests for elastomeric materials have been developed thanks to the pathbreaking study of Rivlin and Thomas[10] (1953) that introduced energy criteria, associating the crack growth rate to the energetic state of the material.

The strain energy release rate, usually called Tearing Energy (T), is defined as the surface energy density required for the propagation of a crack in the material,

$$T = \frac{1}{t}\frac{dW}{dc}, \qquad [1]$$

where dW is the mechanical work necessary to propagate a crack of transverse thickness t along a length dc. This definition can be considered as an extension to elastomers of Griffith's theory[11]. Since the earliest studies Tearing Energy has been considered a material property, since it is valid for a wide range of specimen sizes and geometry.

The first theories have been confirmed by subsequent works of Lake and Lindley[12,13] and Gent et al[14,] demonstrating that tests performed with different samples lead to similar results

in terms of crack growth rate versus tearing energy. In particular, it was reported that experimental data in natural rubber (NR)-based formulations could be interpolated by a quadratic power law equation. Subsequent studies revealed that the exponent of the power law equation can vary, being closely related to compound formulation.[12]

A very general relationship between the crack growth rate *dc/dN* and tearing energy *T* can be written in the form:

$$\frac{dc}{dN} = A \cdot T^{\beta} \qquad [2]$$

where β and *A* are, respectively, the slope and the intercept of the line obtained when eq. [2] is plotted on a bi-logarithmic scale.

One of the geometries usually applied for fatigue crack growth tests is the so-called SENT (*see figure 1*) specimen, made of a thin strip of rubber with high height-to-width ratio. With this geometry a small cut on the side of the specimen is provided as initial crack (c_0).

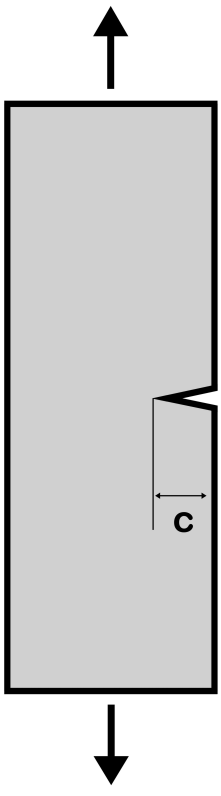

Fig. 1 – SENT specimen geometry

When a tensile load is applied to the edges of the sample, the energetic state at the crack tip is related to the energy and to the crack length through the relationship:

$$T = 2kUc \qquad [3]$$

where U is the strain energy density, c the crack length, and $k = \frac{\pi}{\sqrt{1+\varepsilon}}$ is the strain extension factor, *where ε is the strain*. In this equation the value of T is influenced by the crack length[15,16].

In contrast to SENT, a sample geometry with low height-to-width ratio (fig. 2) creates a zone of equibiaxial stress state, also called pure shear[17], with no edge effect close to the crack tip; as a consequence tearing energy can be considered independent of crack length.

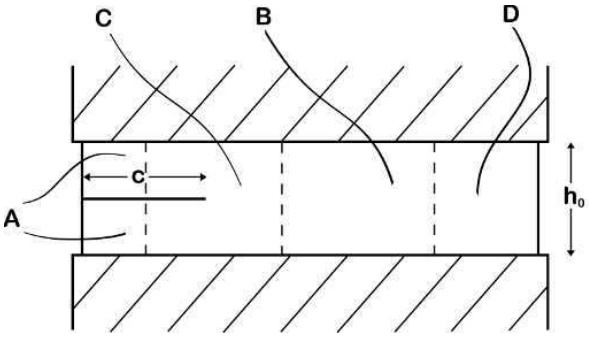

Different state of stress zones	
A	No tension zone
B	"pure shear" zone
C	Zone with complex stress states
D	Zone affected by edge effects

Fig. 2 – Pure shear specimen geometry with indications of the zones at different stress states

The use of this type of sample, when tests are performed in strain control, allows one to keep constant the value of tearing energy during the test, while the crack grows uniformly with the number of cycles.

Referring to figure 2, four regions of different stress states can be recognized within the specimen:

- zone A, not in tension;
- zone B, affected by pure shear stress;
- an intermediate zone C, undergoing complex stress state; and
- final zone D, influenced by edge effects.

The mathematical description used for the calculation of the tearing energy in case of pure shear is:

$$T = U \cdot h_0 \qquad [4]$$

where U is the strain energy density, and h_0 is the unstrained height of the sample. In this case the tearing energy does not depend on the crack length c.

MATERIALS AND METHODS

Crack growth tests have been performed on three different compounds, for which the formulations are reported in Table I. The formulations mainly differed in the elastomer type, NR or synthetic rubber, whereas the other mixing ingredients were kept almost unchanged, apart from minor adjustments to achieve comparable curing rates. All compounds were black-filled with 50 phr of Carbon Black N330 type.

Table I
Model compound formulation (phr)

	SBR	NR	BR
E-SBR 1500	100	-	-
SMR20	-	100	-
High-Cis Nd-BR	-	-	100
N330	50	50	50
ZnO	2	2	2
Stearic Acid	1	1	1
Sulfur	2	2	2
TBBS*	2	1	2
MTBS**	-	-	0.5
6PPD***	1	1	1

* N-tert-butylbenzothiazole-2-sulphenamide; ** 2,2'-Dithiobis(benzothiazole); *** N-(1,3-Dimethylbutyl)-N'-phenyl-p-phenylenediamine

The compounded stock was prepared with a two-stage mixing procedure in a 330 cc Banbury Mixer with a chamber fill factor of 0.7.

In the first, non-productive, stage the initial conditions were 100°C and 100 rpm. The polymer was introduced for first in the chamber, and the filler was added after 2 mins. After 7 min of total mixing time, the compounded stock was discharged.

The subsequent productive stage was carried out at 100°C and 50 rpm. The compound obtained from the nonproductive stage was introduced first in the chamber, and after 2 min, all chemicals (sulphur, curatives etc.) were added. After 5 min of total mixing time, the compound was discharged. Between the two mixing stages and prior to curing, the compounded stock was passed at room temperature in a two-roll mill.

Strip tensile specimens were cured inside a Monsanto fatigue test mold, as specified in ASTM 4482, and then shaped by a die-cutter *to obtain a sharp initial crack*. The same curing conditions were chosen for all compounds (160°C for 15 min, under a pressure of 100 bar). Specimens dimensions were 65 mm height, 13mm width and 1.4mm thickness, with a lateral cut c_0 of 2 mm; these dimensions were selected to provide a width-to-height ratio equal to 10.

Pure-shear samples were prepared using one sheet of model compound reinforced by two sheets of rubber textile composite at the edges to prevent sample slippage and deformation within the clamps (see figure 3 for sample details). Dimensions of the non-reinforced rubber were 15mm height, 150mm width, and 1.4mm thickness; a sharp lateral crack of 20mm was then made on the sample. The assembled sample was then cured in a press as per above.

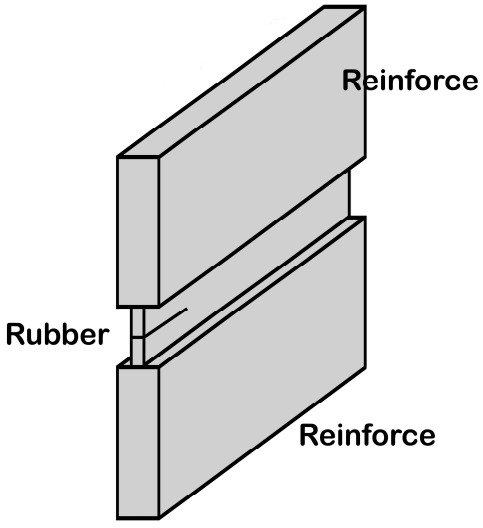

Fig. 3 – Sketch of pure-shear sample.

Crack propagation of cured compounds was determined using a Tear Analyzer machine produced by Coesfeld GmbH & Co., which is capable of measuring the growth of the crack in the rubber specimen through a system of image processing.

III. EXPERIMENTAL RESULTS

PRELIMINARY CASE STUDIES ON PURE-SHEAR TEST

A styrene-butadiene rubber (SBR)-based compound was chosen as case study, to confirm with experimental data the application of a pure-shear stress state within the selected geometry.

Figure 4 shows that the strain energy density (*Utot*) remains nearly constant during testing; thus an average value can be used to calculate Tearing Energy (see equation [4]); the crack length instead increases linearly with the number of cycles; hence the slope can be considered as the crack growth rate (*dc/dN*). The tests were stopped after a crack propagation of few millimeters (typically 5 mm).

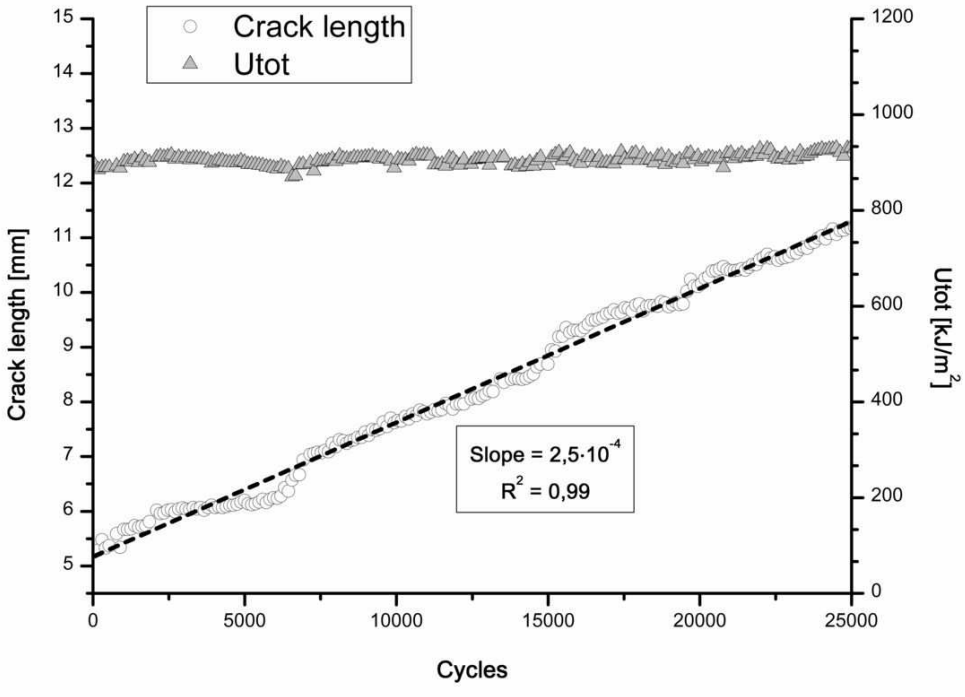

Fig. 4 – Strain energy density (Utot) and crack length during a pure-shear test.

In case of strip-tensile specimens, the characteristic plot of the crack propagation versus the number of cycles is divided in 3 zones (see figure 5-a): crack nucleation (zone 1), crack propagation in steady state (zone 2) and final catastrophic failure (zone 3).

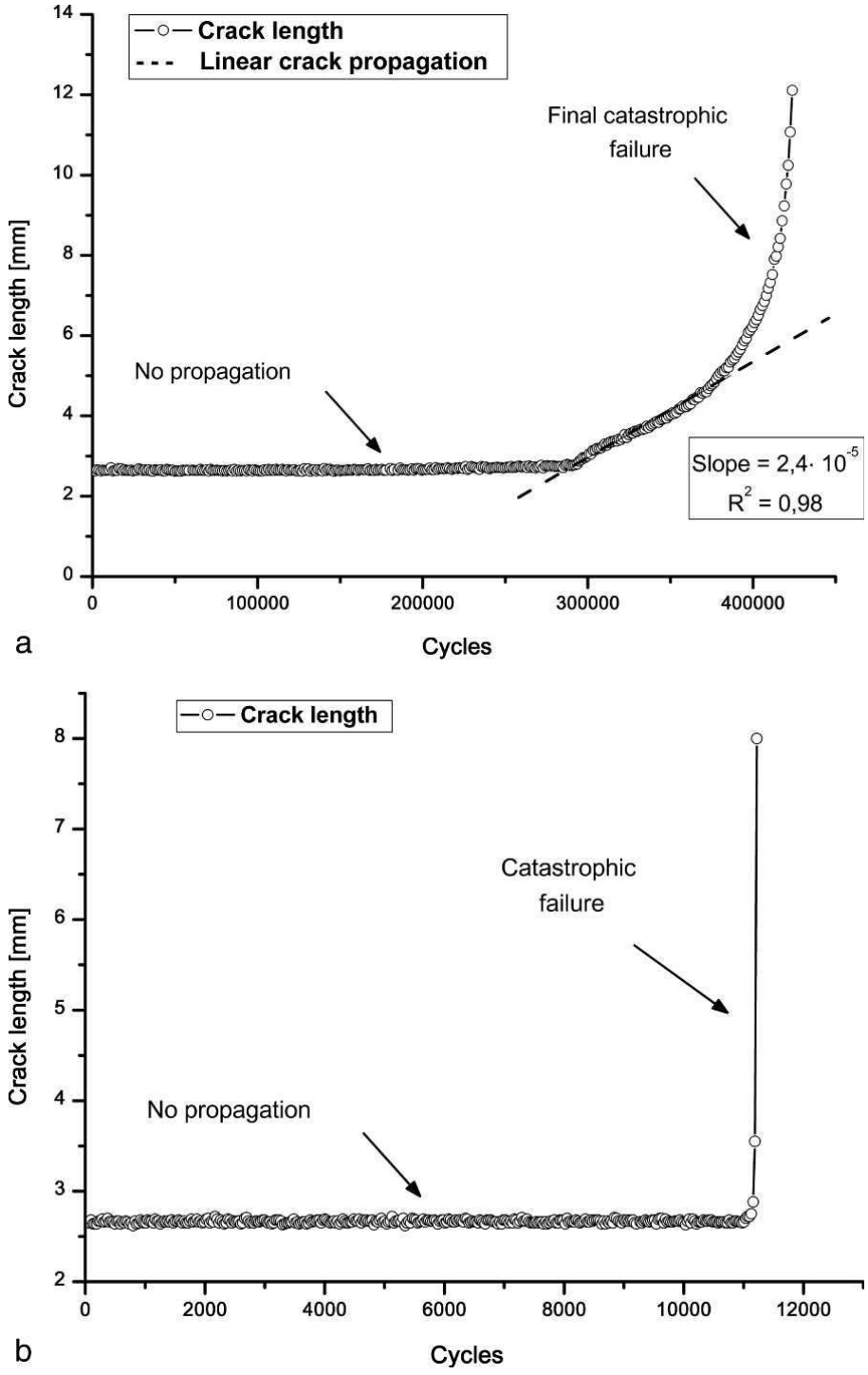

Fig. 5 – Comparison of crack propagation behavior for SBR (a) and BR (b) compound with SENT geometry.

These three zones however cannot always be clearly detected: a typical example is the case of compounds based on BR, where the crack propagates catastrophically, hindering the possibility of properly evaluating *dc/dN* in steady state with subsequent high variability in test results (see figure 5-b). Wherever the slope changes among different zones are not univocally defined, the operator influence on data interpretation could be not negligible; different operators may provide different *dc/dN* values.

In the case of pure shear, the operator influence on data interpretation is significantly reduced because the steady-state crack propagation is clearly detected and observed. Moreover, data analysis can be carried out in automatic mode, and results variability is related only to intrinsic fatigue test variability.

SENT VERSUS PURE SHEAR

During the second phase of this experimental work, the influence of specimen geometry has been evaluated using both strip-tensile and pure-shear specimens; crack propagation tests have been performed on different compound formulations (see Table I) at different waveforms (sine and pulse), and the testing conditions have been chosen, as shown in Table II, so as to evaluate crack propagation behavior in a similar range of tearing energy.

All tests have been performed using strain as control parameter both for SENT and pure-shear samples. The differences in strain level between SENT and PURE SHEAR can be ascribed to the different stress state deriving from different sample geometry.

Table II
Testing conditions for strip-tensile (SENT) vs. pure-shear specimen

	SENT			PURE SHEAR		
Waveform	Pulse 1-10Hz / Sine 10Hz					
Compound	SBR	NR	BR	SBR	NR	BR
Tearing energy (kJ/m^2) range	0.7 → 5.1	1.3 → 5.5	0.8 → 2.7	0.8 → 5.5	0.9 → 5.5	0.5 → 3.1
Strain amplitude (%)	10 → 40	20 → 50	10 → 20	30 → 120	50 → 150	25 → 70

The effect of different waveforms on the crack growth rate has been investigated by comparing a sinusoidal waveform with a frequency of 10 Hz with a pulse waveform. As shown in figure 6, the pulse waveform was generated using a frequency of 10 Hz for the impulse and 1 Hz for the whole cycle, which corresponds to a deformation applied for 0.1 s followed by a dwell time of 0.9 s.

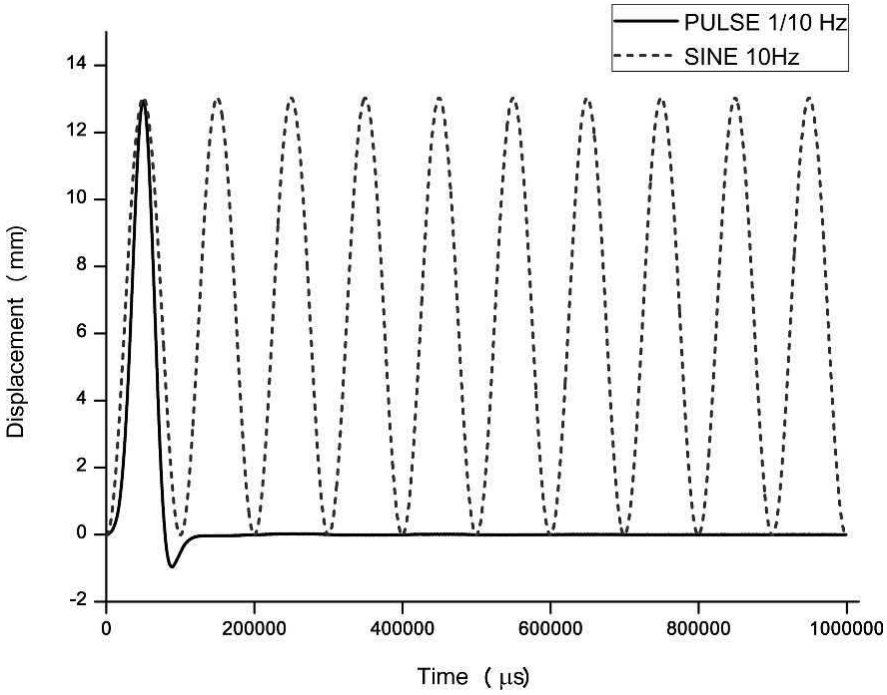

Fig. 6 – Waveforms comparison.

Table III
$R_{RATIO} = P_{MIN}/P_{MAX}$ for each test condition, applied in case of SBR based compound.

SENT		PURE SHEAR	
strain level	R_{RATIO}	strain level	R_{RATIO}
10%	0.033	30%	0.029
20%	0.011	50%	0.006
25%	0.008	80%	0.009
30%	0.005	100%	0.004
40%	0.003	120%	0.003

A minimum value of tensile preload (typically 2N for SENT samples, 5N for pure-shear ones) was always applied to prevent sample bending. This reflects in different R_{RATIO} values for

each test condition, where R_{RATIO} is defined as:

$$R_{RATIO} = \frac{P_{MIN}}{P_{MAX}}, \qquad [4]$$

being P_{MIN} and P_{MAX} the preload and the maximum load, respectively. Table III reports the corresponding R_{RATIO} for each test condition.

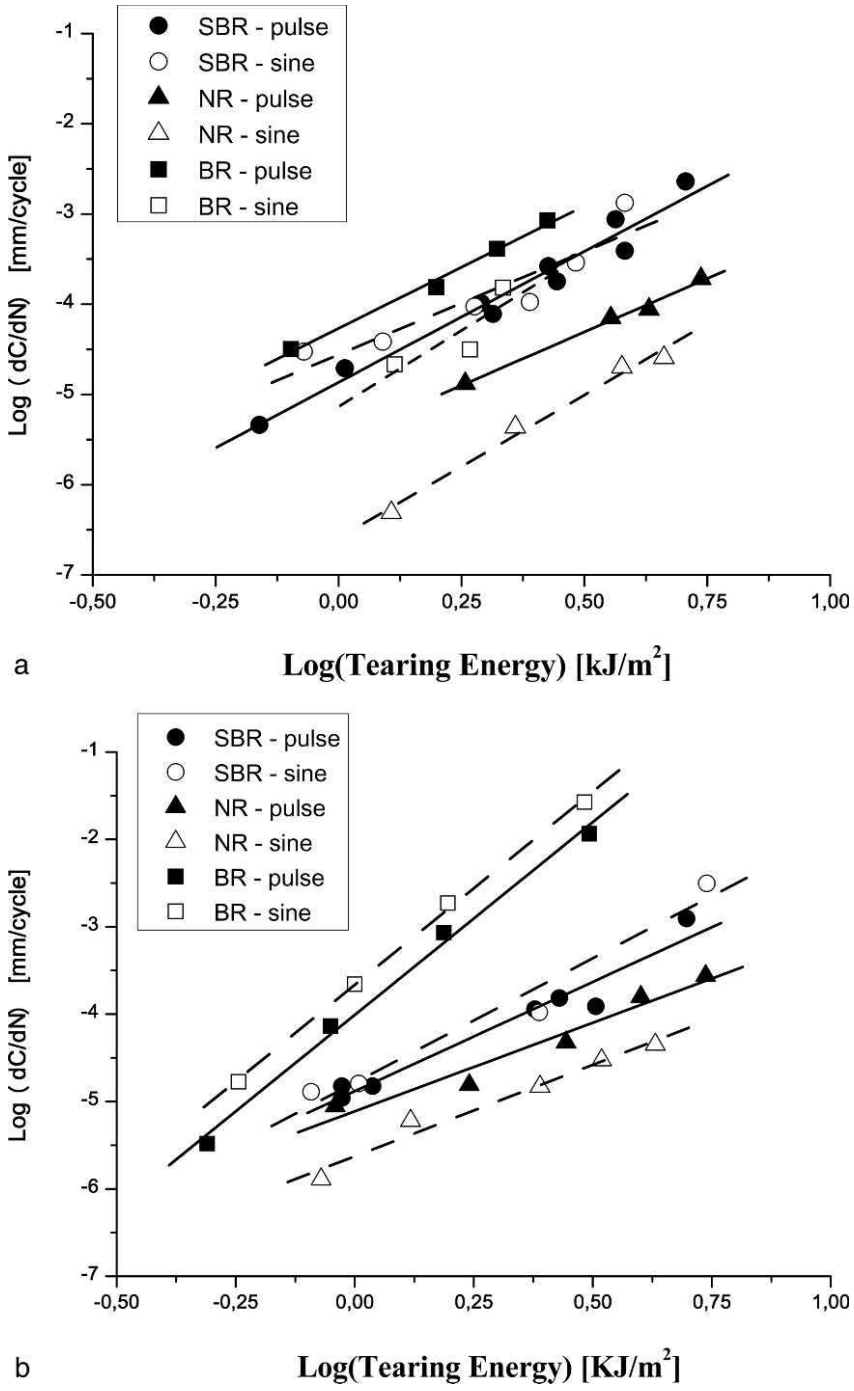

Fig. 7 – Crack propagation of different compounds (dc/dN vs tearing energy) tested with SENT (a) and pure-shear (b) samples.

The crack propagation rate for all compound formulations, obtained by testing pure shear and SENT specimens with both pulse and sine waveforms, is reported in figure 7 as a function of tearing energy, in which each point in figure 7 is the average of 10 different test results.

A similar ranking of crack propagation resistance is achieved for different compounds with both tests (in line with theoretical background[12-14,18]); however, the pure shear testing mode shows more reliable power law dependency and a higher accuracy of results, as evidenced by square deviation factors of R^2 that are always higher than 0.95, whereas in case of SENT the authors experienced some test results with R^2 significantly lower than 0.95 (see Tab. IV).

Table IV
Power Law slope and fitting parameter for SENT and PURE SHEAR

		SENT			PURE SHEAR		
		SLOPE β	Intercept A	R^2	SLOPE β	Intercept A	R^2
BR	Pulse	2.73	$5.35 \cdot 10^{-05}$	0.992	4.43	$9.73 \cdot 10^{-05}$	0.997
	Sine	3.37	$7.34 \cdot 10^{-06}$	0.718	4.42	$2.15 \cdot 10^{-04}$	0.957
SBR	Pulse	3.07	$1.31 \cdot 10^{-05}$	0.984	2.50	$1.31 \cdot 10^{-05}$	0.952
	Sine	2.28	$2.77 \cdot 10^{-05}$	0.851	2.85	$1.63 \cdot 10^{-05}$	0.961
NR	Pulse	2.37	$3.22 \cdot 10^{-06}$	0.993	2.03	$7.68 \cdot 10^{-06}$	0.956
	Sine	3.01	$2.56 \cdot 10^{-07}$	0.980	2.09	$2.36 \cdot 10^{-06}$	0.975

In line with literature background[1,6,12-14,17-19], the pure-shear ranking in terms of crack propagation resistance among different polymer matrixes is a function of tear energy; in particular:

- for high tear energy level: $(dc/dN)_{BR} > (dc/dN)_{SBR} > (dc/dN)_{NR}$, and
- at low tear energy values, the differences in crack propagation speed are reduced: this is a consequence of the higher sensitivity to loading conditions of BR and SBR compounds compared with NR compound (see Tab. IV).

The experiments above show that the effect of the waveform on crack propagation resistance is clearly evident in pure-shear test mode while SENT samples showed high scattering in data

results. Based on above considerations, the authors considered reliable for the further dissertation only the pure shear-test data. In this respect, in the case of NR in particular, the dwell time between two different peaks (equal to zero for sine, 0.9 s in case of pulse) shows how the material ability to increase macromolecular orientation affects the final results. The NR data obtained by using a pulse waveform are always over the equivalent data obtained with a sine waveform.

This characteristic feature could be attributed to NR's ability to recover part of the molecules' orientation during the dwell time in case of pulse waveform with subsequent loss of resistance in the crack propagation direction[20-22]; in the case of BR and SBR formulations, in which the polymers molecules undergo little or no orientation under strain, the linear trend shows that for both materials the sine data are superimposed or close to the pulse ones.

Some additional considerations are related to the power law coefficients (see figure 8): in case of SENT geometry, the slopes obtained with the two waveforms are different (see table IV) and not clearly correlated; in case of pure shear, no significant differences are detectable, and results are strictly related. The analysis on intercepts provides similar information: no correlation between the two waveforms in case of SENT, while a linear tendency is recognizable for pure shear with a shift factor of 0.57.

From a purely practical point of view, it is worthwhile mentioning additional differences between the two testing modes:

1. pure shear testing mode allows overall shorter testing times because fatigue parameters (*dc/dN* and *T*) can be calculated after a crack propagation of just few millimeters, and each sample can be used to measure crack propagation rate at several tearing energy levels;
2. test results obtained in pure-shear mode do not require any interpretation because, contrary to strip-tensile, for pure-shear testing the strain energy density and the crack

propagation speed remain almost constant during the test. In addition to this, data acquisition can be performed in automatic mode.

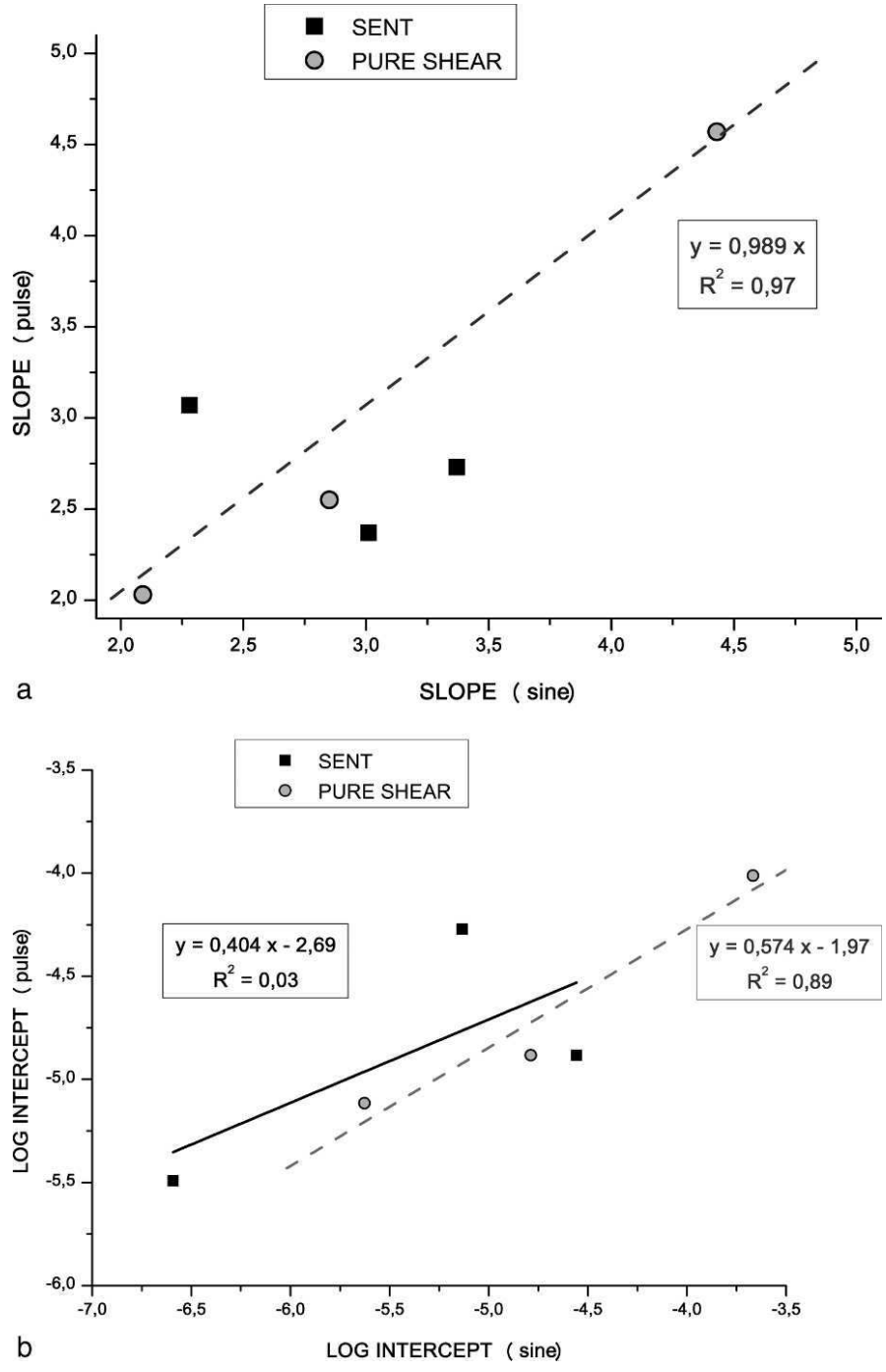

Fig. 8 – Waveform effect on power law's slope (a) and intercept (b) in case of SENT and pure-shear samples.

The added value of pure shear testing mode is especially evident in the case of the BR compound case study, as can be easily observed in figure 9. In Figure 9a, using SENT geometry an initial zone has been observed in which the crack does not propagate; after this

initial zone the crack propagates almost catastrophically. In Figure 9b, by using pure-shear geometry, the crack propagation speed remains constant along the entire test.

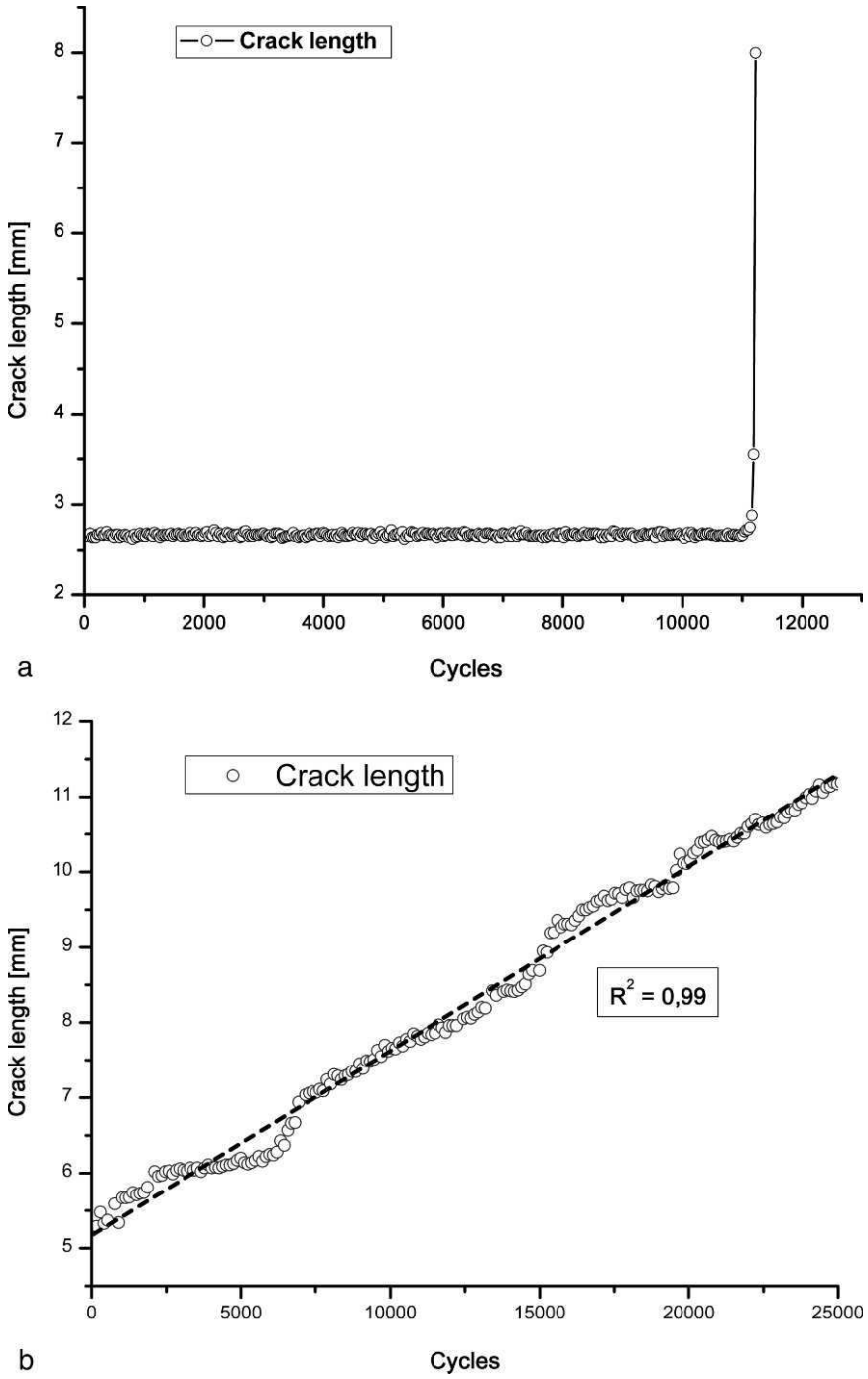

Fig. 9 – Comparison of crack propagation curves of BR compound with SENT (a) and pure-shear (b) samples.

SUMMARY AND CONCLUSIONS

The pure-shear testing mode of different compound formulations provides more reliable

testing results if compared with SENT in terms of *dc/dN* versus tearing energy: $(dc/dN)_{BR} > (dc/dN)_{SBR} > (dc/dN)_{NR}$ within the energy level observed. The use of pure-shear test provides additional valuable advantages:

- crack propagation remains constant during the test, with no influence of crack nucleation;
- tearing energy is independent of the crack length: its evaluation is linked only to strain energy density (constant during the test) and to specimen height (geometric factor);
- no significant differences in power law slope values and linear correlation of the intercept values between sine and pulse waveform (similar consideration cannot be applied to SENT geometry);
- shortened testing times (approximately from days to hours);
- better sensitivity on compound formulation changes.

ACKNOWLEDGEMENTS

The authors would like to thank Bridgestone Corporation for support and for permission to publish this work and Coesfeld GmbH & Co for their support for the machine modification required for pure-shear test.

REFERENCES

1. W. V. Mars, A. Fatemi, Rubber Chem. Technol. 77, 391 (2004)
2. W. V. Mars, A. Fatemi, J Mater Sci, 41, 7324 (2006)
3. D. Hardy, H. Moneypenny, M. Holderied, J. Harris, R. Campion, and G. Morgan, “Low surface area carbon black for tire innerliner”, Paper 2, presented at the 156th Meeting of the Rubber Division, ACS, 22ns-23rd Nov, 1999, Antwerp, Belgium.
4. R. Harbour, A. Fatemi and W. V. Mars, Rubber Chem. Technol. 80, 838 (2007)

5. D. G. Young, Rubber Chem. Technol. 59, 809 (1986)
6. D. G. Young, Rubber Chem. Technol. 58, 785 (1985)
7. U. G. Eisele, S. A. Kelbch and A. J. M. Summer, Crack growth performance of tire compounds, Rubber World, November 1, 1995, pp 38-45.
8. R. Stocek, G. Heinrich and M. Gehde, The influence of the test properties on dynamic crack propagation in filled rubbers by simultaneous tensile- and pure-shear-mode testing, Constitutive Models for Rubber VI, Taylor and Francis Group, London, 2010, pp 345-352.
9. G.Andreini, P.Straffi, S.Cotugno, G. Gallone and G. Polacco, Rubber Chem. Technol. 83, 391 (2010)
10. R.S.Rivlin and A.G. Thomas, J. Appl. Polym. Sci. 2, 291 (1953).
11. A.A. Griffith, Philos.Trans. R. Soc. London, Ser. A 22, 163 (1921).
12. G.J. Lake and P.B. Lindley, Rub. J. 146, 24 (1964).
13. G.J. Lake and P.B. Lindley, J. Appl. Polym. Sci. 9, 1233 (1965).
14. G.J. Lake, P.B. Lindley and A.G. Thomas, J. Appl. Polym. Sci. 8, 455 (1964).
15. C. Timbrell, M. Wiehahn, G. Cook, and A. Muhr, “Simulation of crack propagation in rubber”, presented at Third European Conference on Constitutive Models for Rubber, 15-17 September 2003, London, UK
16. G. Legrain, N. Moes, E. Verron, Stress analysis around crack tips in finite strain problems using the extended finite element method, Int J Numer Meth Eng 63, 2 (2005) pp. 290 - 314.
17. A.G.Thomas, Rubber Chem. Technol. 67, G51 (1989)
18. G.J.Lake, Rubber Chem. Technol. 45, 309 (1972).
19. G. J. Lake and P. B. Lindley, Rubber J. 146 (11), 30 (1964).
20. A.N.Gent, L.Q.Zhang, Rubber Chem. Technol. 75, 923 (2001).
21. S.Berrout, B Huneau, E.Verron, In-situ SEM study of fatigue crack growth mechanism in carbon black-filled natural rubber, Constitutive Models for Rubber VI, Taylor and Francis Group, London, 2010, pp 319-324.
22. J. Zhao, G. N. Ghebremeskel, Rubber Chem. Technol. 74, 409 (2001)